Protoplasma (2014) 251:499–510
DOI 10.1007/s00709-013-0546-3

ORIGINAL ARTICLE

Dissociation of a population of *Pectobacterium atrosepticum* SCRI1043 in tobacco plants: formation of bacterial emboli and dormant cells

Vladimir Gorshkov · Amina Daminova · Marina Ageeva · Olga Petrova · Natalya Gogoleva · Nadezhda Tarasova · Yuri Gogolev

Received: 20 June 2013 / Accepted: 20 August 2013 / Published online: 30 August 2013

Abstract The population dynamics of *Pectobacterium atrosepticum* SCRI1043 (*Pba*) within tobacco plants was monitored from the time of inoculation until after long-term preservation of microorganisms in the remnants of dead plants. We found and characterised peculiar structures that totally occlude xylem vessels, which we have named bacterial emboli. Viable but non-culturable (VBN) *Pba* cells were identified in the remnants of dead plants, and the conditions for resuscitation of these VBN cells were established. Our investigation shows that dissociation of the integrated bacterial population during plant colonisation forms distinct subpopulations and cell morphotypes, which are likely to perform specific functions that ensure successful completion of the life cycle within the plant.

Keywords Plant–microbe interaction · *Pectobacterium atrosepticum* · Viable but non-culturable cells · Bacterial emboli · Heterogeneity of microbial population · Cell ultrastructure

Introduction

Plant–microbe interactions are affected considerably by the conformation of adherent microbial populations, which are quite heterogeneous and consist of morphologically and/or physiologically distinct cell forms. Even in isogenic populations, individual bacterial cells can differ from each other in terms of growth rate, respiratory activity, stress resistance and capacity to respond to specific chemical signals (Anetzberger et al. 2009; Lidstrom and Konopka 2010). Several morphological and physiological variants of bacteria, distinct from typical vegetative cells, have been classified according to their characteristics. These variants include viable but non-culturable (VBN) cells (Roszak et al. 1984; Oliver 1995; Grey and Steck 2001; Gorshkov et al. 2009) and cyst-like rest cells (El'-Registan et al. 1980; Duda et al. 1982; Muliukin et al. 1996; Suzina et al. 2004; Kussell and Leibler 2005; El'-Registan et al. 2006; Muliukin et al. 2008). Biofilms make a substantial contribution to determine the conformations and other properties of microbial populations. Biofilms comprise a group of bacterial cells that are connected to each other through an extracellular matrix (Ramey et al. 2004; Stoodley and Stoodley 2009). Bacteria within a biofilm community differ from planktonic cells in terms of their stress resistance and virulence towards hosts (Matz et al. 2005; Christensen et al. 2007; Manos et al. 2009). Understanding of the sources and implications of physiological heterogeneity of bacteria is of fundamental relevance to a number of fields, such as ecology, medicine and plant pathology. However, the dynamics of microbial populations within higher organisms, e.g. host plants, are not well documented.

Bacteria that interact with plants may colonise various tissues of their host, such as parenchyma or xylem tissues. These tissues have different physical, chemical, nutritional and immune properties. For instance, given that mature xylem vessels are non-living cells, they lack the capacity to mount a hypersensitive defence reaction (Huang et al. 1975). Compared with the contents of parenchyma and phloem cells, xylem sap has fewer growth-promoting nutrients and a high rate of diffusion that is driven by the flow of water. Although more attractive to pathogens due to high nutrient content, parenchymatous cells are more active against pathogen invasion than xylem vessels. As a result, bacteria that colonise different host tissues, even within a single plant, find themselves in distinct conditions.

Handling Editor: Friedrich W. Bentrup

V. Gorshkov (✉) · A. Daminova · M. Ageeva · O. Petrova · N. Gogoleva · N. Tarasova · Y. Gogolev
Kazan Institute of Biochemistry and Biophysics, Kazan Research Center, Russian Academy of Sciences, Lobachevsky Street 2/31, 420111 Kazan, Russia
e-mail: gvy84@mail.ru

This, in turn, may induce diversification in the physiology of the integrated microbial population *in planta*.

Notwithstanding these insights, fluctuations in the structures of bacterial populations in systems as heterogeneous and dynamic as those found in plants are far from being understood. In the study reported herein, we tackled the challenge of better understanding morphological and physiological diversification of bacteria within plants by analysing the interaction of tobacco plants with *Pectobacterium atrosepticum* SCRI1043 (*Pba*), a causative agent of soft rot and potato "blackleg". Although tobacco is not a natural host of *Pectobacterium*, it has been used extensively as a model system for studying various aspects of the *Pectobacterium*–plant interaction (Cui et al. 1996; Mäe et al. 2001; Ger et al. 2002; Kim et al. 2011). Results of our preliminary experiments indicated that, unlike potato plants, individual tobacco plants do not vary much in terms of the symptoms of *Pba*-caused infection. The relative homogeneity in symptoms is a significant advantage when analysing the population structure of the pathogenic bacteria.

Pba is one of the most extensively studied phytopathogens. This is particularly true now that its genomic sequence has been determined (Bell et al. 2004). Many virulence factors and the mechanisms by which their production is regulated have been elucidated for *Pba* and related species (Collmer and Keen 1986; Liu et al. 1999; Tang et al. 2006; Barnard et al. 2007; Mattinen et al. 2007; Liu et al. 2008; Lin et al. 2010). However, although much is understood about *Pba* virulence factors and their regulation, little is known about how this pathogen "behaves" in the heterogeneous environment within plants and how this behaviour permits effective colonisation of the plant.

The aim of the investigation reported herein was to trace the changes in the structure of a bacterial population *in planta* through the entire period of interaction between the bacteria and the plant. Ultrastructural features of the bacterial cells that have colonised different plant tissues were characterised at different stages of the interaction, starting from the time of inoculation and continuing until long-term preservation of microorganisms in the remnants of dead plants. Viable but non-culturable *Pba* cells were recovered from the remnants of dead plants. We also found and characterised peculiar structures that totally occlude xylem vessels, which we have named bacterial emboli. This investigation demonstrates that bacterial populations dissociate during plant colonisation. This generates distinct subpopulations, which are likely to perform specific functions that enable bacteria to complete their life cycle within the plant.

Materials and methods

Plant growth conditions

Nicotiana tabacum cv. Havana plants were grown axenically in test tubes in a growth chamber with a 16-h light/8-h dark cycle photoperiod. Seeds were surface-sterilised using diluted bleach (0.8 % of active chlorine) and 1 % sodium dodecyl sulphate for 30 min, washed seven times with sterile distilled water, then transferred to Murashige and Skoog medium (MS) (Murashige and Skoog 1962) in Petri dishes. Ten-day-old seedlings were transferred to individual flasks containing MS.

Inoculum preparation and plant inoculation

A strain of *Pectobacterium atrosepticum* SCRI1043 (formerly *Erwinia carotovora* ssp. *atroseptica* SCRI1043) was cultured in Luria–Bertani (LB) broth (Sambrook et al. 1989) on a rotary shaker (180 rpm) at 28 °C until the early stationary phase (2×10^9 colony-forming units (CFU ml^{-1})). Six to seven weeks after planting, the stems of tobacco plantlets were inoculated with inoculum containing 2×10^7 CFU ml^{-1}. Sterile water or bacterial suspension containing 2×10^5 cells were placed as 10-μl drops on the surface of the plant stem without wounding the tissue.

Light and transmission electron microscopy

Sections of tobacco stem (0.5–0.8-mm thick) were excised using a sterile razor blade, at 18 h or 2, 3 or 9 days after inoculation. The samples were fixed in 2.5 % glutaraldehyde prepared in 0.1 M phosphate buffer (pH 7.2) at 4 °C overnight, washed three times (15 min each) with 0.1 M phosphate buffer containing sucrose (68 g l^{-1}), and post-fixed by incubation in 1 % (*w*/*v*) osmium tetroxide in the same buffer with sucrose (25 mg ml^{-1}) at 4 °C for 4 h. The samples were dehydrated by passage through a graded ethanol series (30, 40, 50, 60, 70, 80, 90 and then 96 % ethanol), before being transferred to 100 % acetone and propylene oxide. Then the samples were immersed in Epon resin (Fluka) that contained propylene oxide added in the proportions (*v*/*v*) 1:2, 1:1 and 2:1, with each step involving a 12-h incubation. The samples were then embedded in pure Epon resin.

Semi-thin sections (ca. 2-μm thick) were mounted on microscope slides and stained with 1 % (*w*/*v*) methylene blue. The sections were examined using a laser confocal fluorescent microscope (LSM 510 Meta; Carl Zeiss, Jena, Germany) operated with bright field illumination.

Ultrathin sections (ca. 300 nm) were prepared using a glass knife with an ultramicrotome (LKB-8800, Sweden), mounted on copper grids and stained with 2 % aqueous uranyl acetate (*w*/*v*) for 20 min and Reynolds' lead citrate (Reynolds 1963) for 7 min. Some samples were stained according to Thiéry (1967). The sections were mounted on gold grids and treated sequentially with 1 % aqueous periodic acid for 30 min, 0.2 % thiocarbohydrazide in 20 % acetic acid for 2 h and 1 % aqueous silver proteinate for 30 min in the dark. The sections were examined using a transmission electron microscope

(JEM-1200 EX, Jeol, Japan) operated at an accelerating voltage of 80 kV.

Determination of Pba CFU titre in infected tobacco plants

Plant shoots, roots or remnants were weighed separately after 1, 2, 3, 9, 30 and 60 days after inoculation and ground in mortars with two volumes (*w*/*v*) of AB medium (1 g of NH_4Cl, 0.62 g of $MgSO_4 \cdot 7H_2O$, 0.15 g of KCl, 0.013 g of $CaCl_2 \cdot 2H_2O$ and 0.005 g of $FeSO_4 \cdot 7H_2O$ per litre, pH 7.5). The number of CFUs was determined by the plating of serial 10-fold dilutions of the obtained suspensions onto 1.5 % LB agar. The plates were incubated at 28 °C for 2 days before the CFUs were counted. Bacterial densities were expressed as the log CFU per gram of colonised stem or root tissue.

Determination of Pba genome copy numbers in infected tobacco plants

Genome copy (GC) numbers were determined by means of real-time polymerase chain reaction (PCR) with respect to calibration curves as was described previously (Gorshkov et al. 2010). Real-time PCR was performed using the TaqMan detection method. The primers and probes used were designed using Vector-NTI version 9 software (Invitrogen) and synthesised by Syntol (Moscow, Russia). Primers (expIF 5′-GGAATTAGCGTAGTTGAACAAGGTCTG-3′, expIR 5′-GCCACTGCTTCAATTCATTGCTC-3′, EcaF 5′-GATGATTCTTTTGAGTCATGTTTAC-3′, EcaR 5′-GACACTTTTCGCAGGCTACCACG-3′) and probes (expI TaqMan probe 5′-(FAM-C)CCACTGCGG(T-BHQ1)TAATACGACGAGCCAAAGC-3′, Eca TaqMan probe (FAM-T)GTGTCAA(T-BHQ1)GAGTCTCTCAAATAATCGCAGCGC) for the gene *expI* and the 16S–23S rRNA intergenic spacer were specific for *Pba* SCRI1043 (NCBI GenBank accession number NC_004547). The reaction mixture contained 1 × PCR buffer (67 mM Tris–HCl, pH 8.8, 17 mM $(NH_4)_2SO_4$, 2.5 mM $MgCl_2$, and 0.1 % Tween 20), 100 mM of each dNTP, 0.04 U of Taq DNA polymerase (Sileks), 0.2 mM of each primer and TaqMan probe. The thermal cycling conditions used for PCR involved heating to 94 °C for 2 min, followed by 45 cycles at 94 °C for 10 s and 60 °C for 1 min. Changes in fluorescence emission were detected using an IQ-4 quantitative PCR system (Bio-Rad). The amount of fluorescence was plotted as a function of PCR cycle using iCycler iQ Optical System Software version 3.1 (Bio-Rad). The amplification efficiency (*E*) for all primers was determined using a dilution series of a DNA pool. A value of 5.5 fg of *Pba* DNA (5,064 kb) was accepted as one GC. The DNA concentration was determined using a Qubit fluorometer (Invitrogen, USA).

Genome copy numbers were analysed in cell lysates that had been diluted 10^N-fold in deionised water. Shoots or remnants of the inoculated plants were weighed and ground separately in mortars with two volumes (*w*/*v*) of AB medium. Aliquots of the suspensions generated (200 μl) were used to prepare cell lysates in 2 % Triton X-100 (*v*/*v*) at 100 °C, as described previously (Gorshkov et al. 2010). Cell lysates from early stationary-phase cultures were used as a positive control. Genome copy numbers in the PCR reaction mixture ranged from 10^2 to 10^7, and the calibration curve was linear in this range. The GC numbers were determined 1, 2, 3, 9, 30 and 60 days after the plants had been inoculated with bacteria. Bacterial densities were expressed as a log GC per gram of plant tissue.

Procedures for resuscitation of Pba VBN cells

Thirty days after the plants were inoculated with *Pba*, plant remnants were weighed separately and ground in a mortar with two volumes (*w*/*v*) of AB medium. Aliquots of suspensions were seeded on LB agar to confirm the absence of CFUs recovered before the resuscitation procedure. The debris was then washed twice and resuspended in the initial volume of AB. The obtained suspensions were (1) plated as serial 10-fold dilutions onto 1.5 % LB agar; (2) enriched with either a 1/10 dilution of plant extract or a 1/10 dilution of LB broth, incubated at 28 °C for 2 days, and then plated on LB agar; or (3) used to inoculate sterile tobacco plants. The inoculated plants were tested for the presence of *Pba* CFUs 2 and 7 days after inoculation. A fourth protocol (4) involved freezing the plant remnants at −18 °C and keeping them for a month. After they were thawed for 2 h, the remnants of each plant were divided in half. One half was ground, washed in AB and plated immediately onto LB agar, and the other half was incubated at room temperature for 2 days before being plated into LB agar. All resuscitation procedures were performed under sterile conditions.

Plant extract was prepared by homogenisation of 10 g of sterile tobacco shoots in 25 ml of deionised water using a blender. The mixture was incubated for 2 h at 4 °C with gentle agitation and then centrifuged at 10,000×*g*, 4 °C, for 20 min. The supernatant was further clarified by filtering through a 0.2-μm filter, followed by ultrafiltration (Ultra-15 centrifugal filter device, Millipore). The filtrate was lyophilised, dissolved in deionised water, filter-sterilised and stored at −18 °C before use.

Statistical analysis of results

In each of the four independent experiments, four biological replicates were assayed, each with four technical replicates. The data are presented as medians ± 0.975 and 0.025 percentiles of all four independent experiments. The significance of the differences among the results of each test and the relative control values was determined using Student's *t* test, with $P <$

0.05 considered to be statistically significant. The electron microscopy data comprise the reproducible results of two independent experiments, each with three biological replicates.

Results

Growth of Pba in tobacco plants

The first symptoms of disease in most of the tobacco plants inoculated with *Pba* became visible on either the first or second day after inoculation. The primary symptoms involved local tissue maceration at the inoculation site; the tissue damage extended both upward and downward over time (Fig. 1). By 4 to 5 days after inoculation, the entire plant was macerated (Fig. 1c). During the first 3 days after plant inoculation, the bacterial population increased by more than four orders of magnitude, as measured by both plating and real-time PCR (Fig. 2). During the period from 3 to 9 days post-inoculation, bacterial cell number in inoculated plants remained stable. No CFUs were recovered from plant remnants 20, 30 or 60 days after plant inoculation. However, GC values remained relatively high 20, 30 or 60 days after inoculation (Fig. 2). No colonies were recovered and no real-time PCR signal was detected from plants that were not inoculated.

VBN cells of Pba in remnants of tobacco plants

Given that the CFU values of *Pba* in plant remnants fell to undetectable levels, although the GC value in these tissues remained relatively high (Fig. 2), we considered the possibility that the bacterial cells transitioned to the VBN state after the death of the plant. To verify this, several procedures for bacterial cell resuscitation were performed ("Materials and methods" section), two of which were effective. The first approach involved homogenisation of dead plants (30 days after inoculation) for which a failure to detect CFUs had been confirmed, then washing the homogenate twice in carbon-deficient medium and seeding the suspension on solid LB medium (Gorshkov et al. 2009). This procedure restored CFU titre from 0 to 8.0×10^2 to 3.2×10^6 CFU g^{-1} of plant debris, but only in 3 of the 26 plants analysed. The second procedure involved an additional step: before homogenisation and washing, the samples were kept frozen (−18 °C) for a month. Immediately after thawing for 2 h and washing twice in carbon-deficient medium, 5 of the 30 samples had CFU titres restored from 0 to 5.3×10^3 to 1.7×10^6 CFU g^{-1} of plant debris. When, after thawing, samples were incubated at room temperature for 2 days and then washed twice, an additional five samples showed restoration of the CFU values. Altogether, CFU values were restored in 10 of the 30 samples of frozen plant remnants.

When resuscitation occurred, 10 randomly chosen colonies recovered from each sample were confirmed to be *Pba* by means of PCR with *Pba*-specific primers listed above ("Materials and methods" section). The PCR products obtained from five samples were sequenced. All of them had *Pba*-specific sequence (data not shown). Moreover, several colonies recovered after cell resuscitation were transferred into fresh LB medium, incubated overnight, and the obtained cultures were used to inoculate tobacco plants. All these cultures displayed virulence same as the initial ones (data not shown).

Pba in tobacco plants: ultrastructural analysis

Early stages of tobacco colonisation by Pba

Neither bacterial cells nor any of the structural abnormalities described below were found in uninoculated tobacco plants (data not shown). Eighteen hours after plant inoculation, individual bacterial cells with typical ultrastructure (Gorshkov et al. 2009) were observed at the sites of inoculation in the lumens of xylem vessels (Fig. 3a) and in the parenchyma (Fig. 3b–e). Within the parenchyma tissue, *Pba* cells were observed both in the apoplast (Fig. 3b) and inside the plant cells (Fig. 3c–f). Halo zones (an electron-lucent layer around the *Pba* cells), which presumably corresponded to the bacterial capsules, could be observed against the background of the plant cell cytoplasm (Fig. 3c). Cellular ultrastructure varied between different parenchyma cells infected with bacteria. In some of these cells, there was no substantial alteration of the cytoplasm structure, and formation of osmiophilic globules was evident in the vacuole (Fig. 3c). In others, the cytoplasm became more loosened and the tonoplast underwent substantial structural alterations (Fig. 3d). In certain parenchymal cells, the tonoplast could not be discerned and the organelles were visibly damaged (Fig. 3e). In other parenchymal cells, in which the cytoplasm and

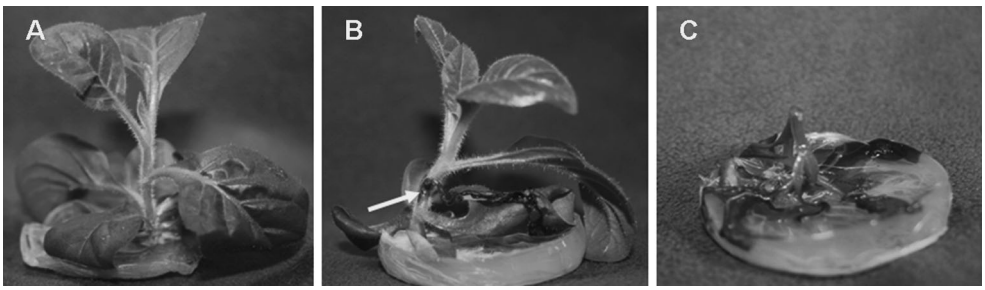

Fig. 1 Tobacco plants infected with *Pectobacterium atrosepticum* SCRI1043. **a** Uninoculated (control) plant; **b** 2 days after inoculation, note the maceration zone on the stem (*arrow*); and **c** 5 days after inoculation

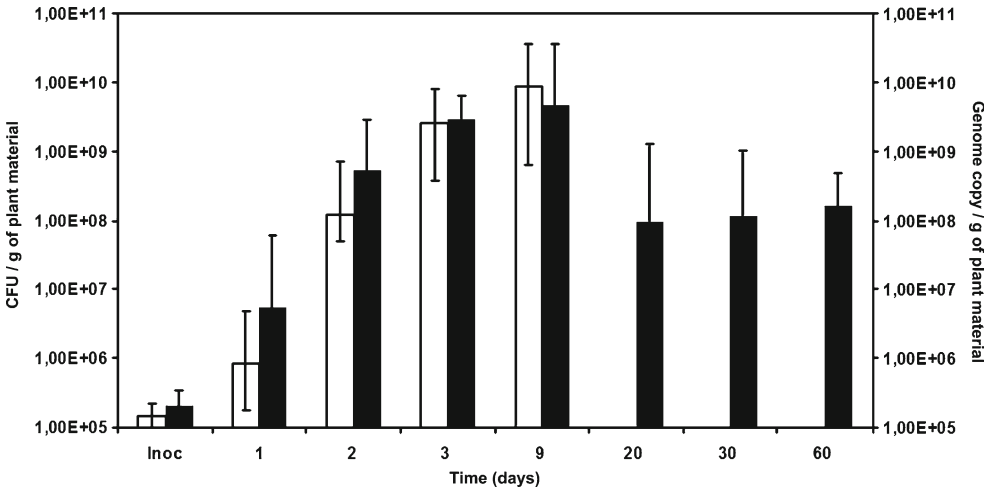

Fig. 2 Growth of *Pectobacterium atrosepticum* SCRI1043 in tobacco plants, showing CFU values (*white columns*) and genome copy values (*black columns*) per gram (fresh weight) of plant material (shoots or their debris). *Inoc* represents the inoculum quantity. The *values* represent medians of four independent experiments ± 0.975 and 0.025 percentiles

organelles were destroyed and there was evidence of invagination and vesicularisation of the plasmalemma, bacteria were entrapped within the membrane system (Fig. 3f). No ultrastructural modifications of xylem vessels were apparent 18 h after inoculation of the plants.

Colonisation of tobacco xylem vessels by Pba: formation of bacterial emboli

During the early stages of vessel colonisation, when few bacteria were observed in the lumen, granular substances were released from the plant cell wall (Fig. 4a). These substances, which were either free or attached to bacteria, were unlikely to be bactericidal given that no bacterial damage was noted at this stage. As the number of bacteria within the lumens of the vessels increased, the granular substances became more and more dispersed, resulting in the formation of a gel that contained many bacteria. A sequential outline of the stages of gel formation is presented in Fig. 4 a–c.

After gel formation and the increase in the number of *Pba* cells within the vessels, the bacterial cells aligned along the longitudinal axis of the xylem vessel (Fig. 4d). In addition to

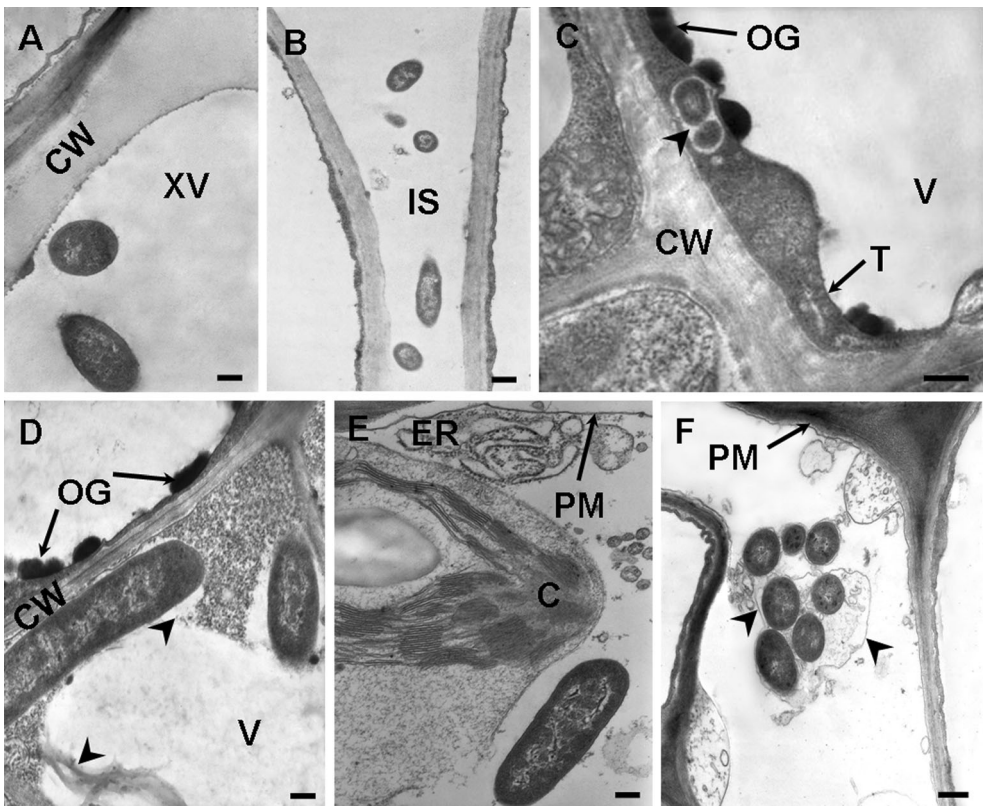

Fig. 3 Transmission electron micrographs of tobacco stems infected with *Pectobacterium atrosepticum* SCRI1043 (*Pba*) (inoculation area, 18 h after inoculation). **a** *Pba* cells in the xylem vessel, bar=0.2 μm; **b** *Pba* in the intercellular space (*IS*), bar=0.5 μm; **c** *Pba* in the cytoplasm of parenchymatous cell, note the halo zone around bacterial cells (*arrowhead*) and osmiophilic globules (*OG*) in the vacuole, bar=0.2 μm; **d** *Pba* in the cytoplasm of parenchymatous cell, note the ruptured tonoplast (*arrowheads*), bar=0.2 μm; **e** *Pba* in parenchymatous cell, note the degradation of chloroplast and endoplasmic reticulum, bar= 0.2 μm; and **f** *Pba* covered with membranous structures (*arrowheads*) inside the parenchymatous cell, bar= 0.5 μm. *CW* plant cell wall, *PM* plasma membrane, *T* tonoplast, *V* vacuole, *C* chloroplast, *ER* endoplasmic reticulum

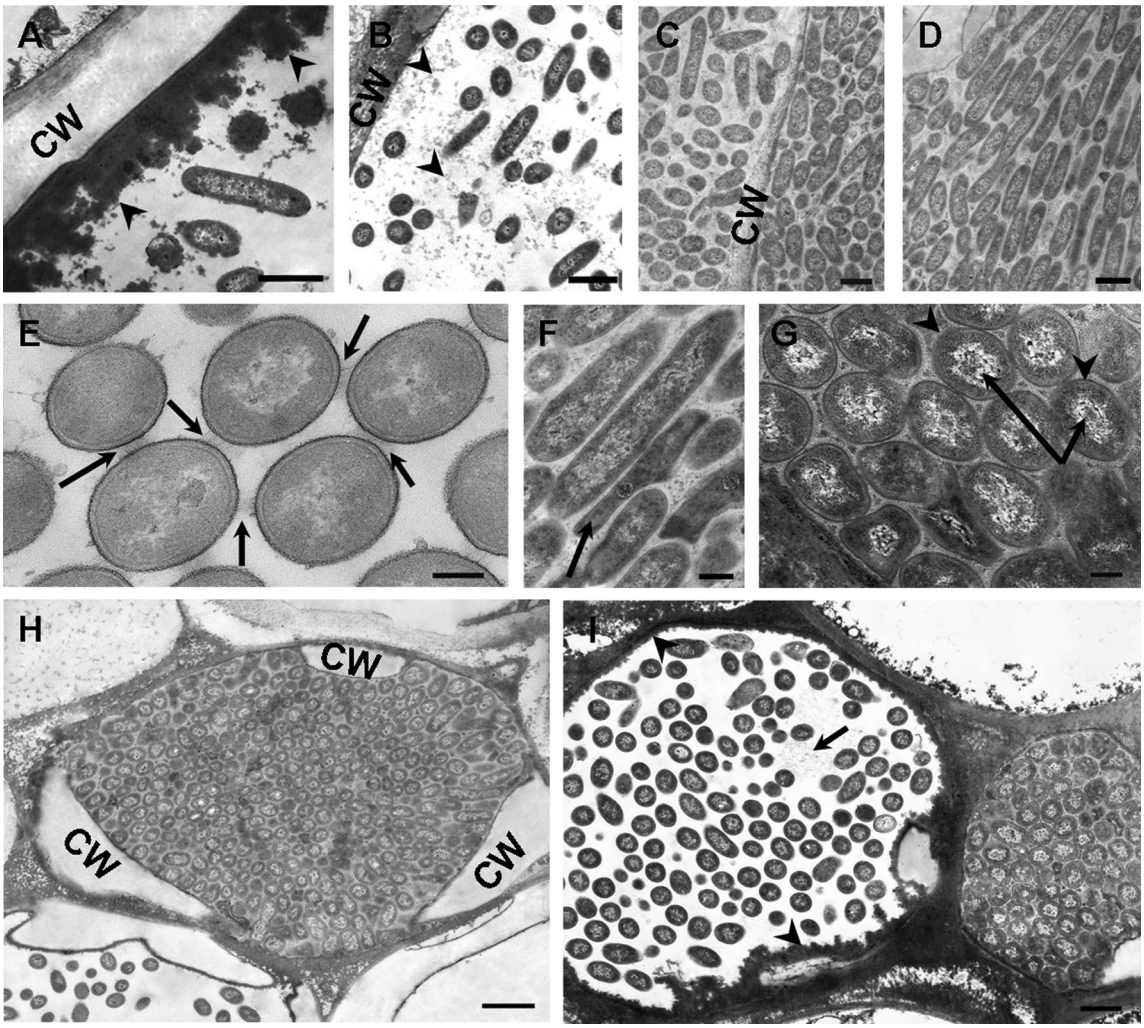

Fig. 4 Formation of bacterial emboli in xylem vessels of tobacco stems infected by *Pectobacterium atrosepticum* SCRI1043 (*Pba*) 2–3 days post-inoculation (dpi). Transmission electron micrographs show different stages of vessel colonisation (**a**–**d** and **f** longitudinal sections; **e**, **g**–**i** cross sections). **a** Release of granular substances (*arrowheads*) from the cell wall of xylem vessel colonised by *Pba*, bar=1 μm; **b** dispersion of the granular substances (*arrowheads*), bar=1 μm; **c** formation of the gel, note the different density of the gel in two adjacent vessels, in which different amounts of bacteria are localised, bar=1 μm; **d** alignment of *Pba* cells in the longitudinal orientation in the xylem vessel, bar=1 μm; **e** pilus-like structures on the bacterial surface, note the connection between neighbouring *Pba* cells via pilus-like structures (*arrows*), and this sample was stained according to the Thiery method, bar=0.2 μm; **f** deformation of bacterial cells (*arrow*) during formation of the bacterial embolus, bar=0.2 μm; **g** ultrastructure of the *Pba* cells contributing to the formation of an embolus, note the electron-dense peripheral cytoplasm layer (*arrowheads*) and the electron-transparent central zone containing nucleoids (*arrows*), bar=0.2 μm; **h** bacterial embolus totally occluding the xylem vessel, note that on the stem cross section, bacterial cells are cut transversely, so they align the longitudinal axis of the vessel, bar=2 μm; and **i** different stages of bacterial emboli development in two adjacent xylem vessels: to the left is the release of granular substances from the cell wall of xylem (*arrowheads*) and formation of the gel (*arrows*), while to the right is the formed embolus, bar=1 μm. *CW* plant cell wall

the formation of the gel substance, pilus-like structures were formed on the bacterial surface connecting individual cells with each other (Fig. 4e). Pilus-like structures were not distributed across the entire bacterial surface but formed locally in the region of the shortest distance between neighbouring cells. Such pilus-like structures may provide the attachment of the bacteria to each other and therefore contribute to the occlusion of the xylem vessel. The *Pba* cells were packed tightly within the vessels, causing some of the cells to become deformed (Fig. 4f). As a result, peculiar structures were formed in the xylem vessels of infected plants. We termed these structures “bacterial emboli”. Bacterial emboli entirely occluded xylem vessels (Fig. 4g–i). Bacterial cells within the emboli acquired a specific morphology, which was distinct from that formed by cells that colonise the parenchyma or cells cultured in vitro. The cells within bacterial emboli had a very electron-dense peripheral cytoplasm layer and electron-transparent central zone (Fig. 4g). Different stages of formation of bacterial emboli could be observed within the same tissue section (Fig. 4i).

After plant death, bacterial emboli underwent significant structural alterations and were dispersed. The matrix of

bacterial emboli disintegrated, and cells that were adpressed against each other in the bacterial emboli became separated (Fig. 5a, b). The bacterial cytoplasm became more loosened and uniform; the aggregation of the cytoplasm was not observed. Ribosomes were distributed evenly in the cytoplasm. Some cells were plasmolysed, and the nucleoids of bacterial cells could barely be discerned (Fig. 5b, c).

Colonisation of tobacco parenchyma by Pba

Parenchyma was actively colonised by *Pba* within 2–3 days after inoculation. In the parenchyma, most of the *Pba* cells were located in the intercellular spaces (Fig. 6a, b) and inside disturbed parenchymatous cells (Fig. 6a). Bacteria had a typical ultrastructure (Fig. 6b), and no complex bacterial communities, such as biofilms, bacterial emboli or aggregates, were observed in the parenchyma. Most of the plant cell organelles were destroyed. Sometimes, apposition of plant cell walls was apparent (Fig. 6b).

After plant death (9 days post-inoculation), the subpopulation of *Pba* cells that had colonised the parenchyma became heterogeneous (Fig. 6c, d). Some of the bacterial cells were plasmolysed to different extents and showed evidence of clearing of the cytoplasm, which made it difficult to discern the nucleoid. The ultrastructural features of these cells resembled those of VBN *Pba* cells that were previously characterised in vitro (Gorshkov et al. 2009). Other cells had a non-uniform cytoplasm with an electron-dense peripheral layer and a more electron-transparent inner layer, which contained the nucleoid (Fig. 6d).

Expansion of Pba in tobacco plants

To investigate the peculiarities of the expansion of *Pba* in tobacco plants, we analysed sections of infected plants at various distances below the zone of macerated tissue. Single bacteria were rarely seen in the parenchyma of the symptom-free zone 3–5 mm below the macerated area, and no bacteria were observed in the parenchyma beyond 5 mm from the site of maceration. Groups of bacteria were sometimes detected in parenchymatous cells, but only in those adjacent to xylem vessels (Fig. 7a, b). In the area below the macerated zone, osmiophilic globules formed in parenchymatous cells (Fig. 7c). These globules had never been observed in either plant cells in macerated zones that had been invaded extensively by *Pba* cells or in plants that had not been inoculated.

In contrast to the parenchyma, xylem vessels were colonised extensively by *Pba* in the zone more than 1 cm below the site of necrosis (Fig. 7a, b). Bacterial emboli were visible within this zone. Migration of bacteria to the neighbouring parenchymal cells, which was caused by the destruction of plant cell wall, was observed (Fig. 7a, b). Together, these observations indicate

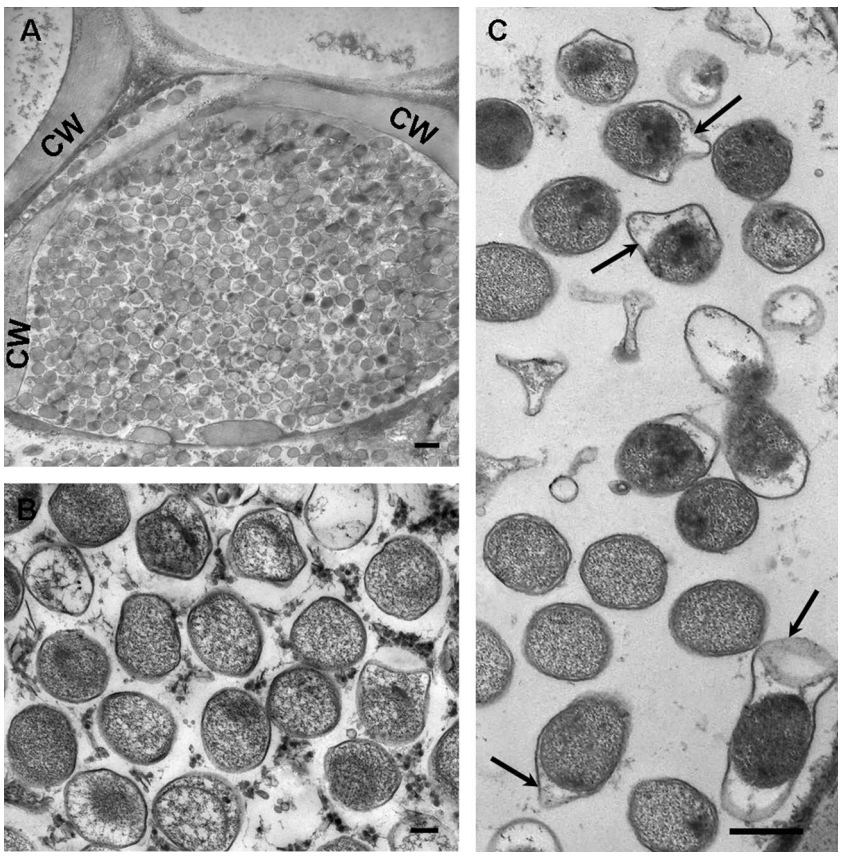

Fig. 5 Dispersion of bacterial emboli in the xylem vessels of tobacco stems infected by *Pectobacterium atrosepticum* SCRI1043 (*Pba*), transmission electron microscopy. **a** Bacterial embolus 6 dpi, bar=2 μm; **b** loosening of the matrix of bacterial embolus, note the more uniform cytoplasm in bacterial cells compared to the ones found within bacterial emboli 3 dpi (Fig. 3g), bar=0.5 μm; and **c** complete dispersion of bacterial embolus, note the plasmolysis in some of the cells (*arrows*), bar= 0.5 μm. *CW* plant cell wall

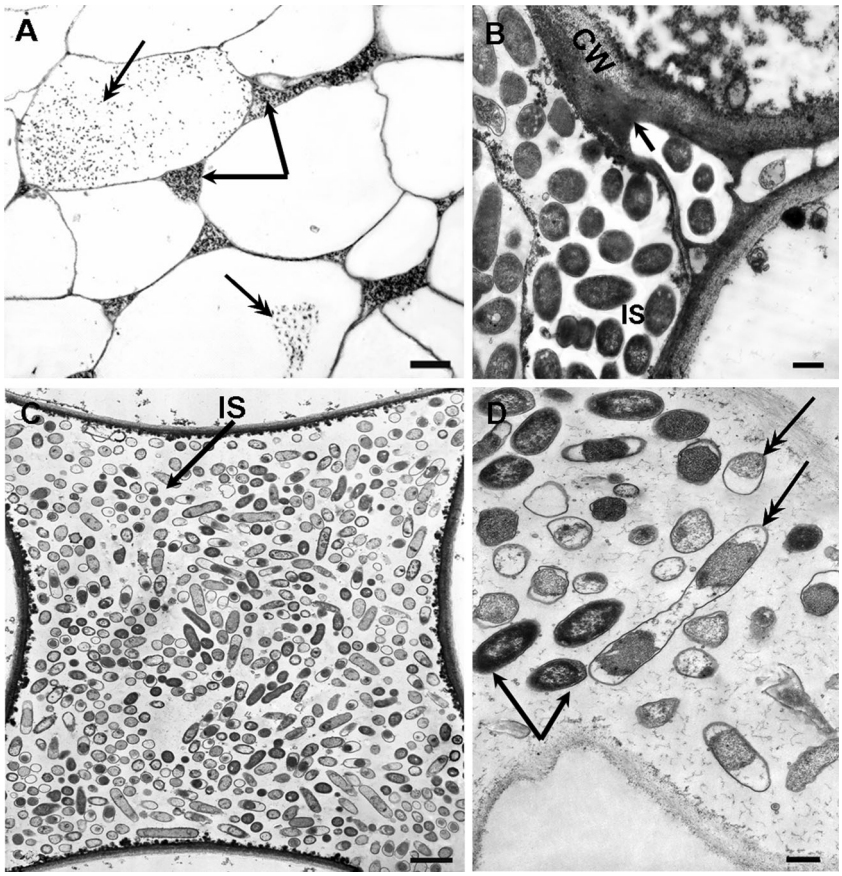

Fig. 6 Colonisation of parenchyma by *Pectobacterium atrosepticum* SCRI1043 (*Pba*) at 3 dpi (**a**, **b**) and 9 (**c**, **d**) dpi. **a** Light microscopy; **b**–**d** transmission electron microscopy. **a** Bacteria in the intercellular spaces (*arrows*) and inside the parenchymatous cells (*double arrows*), bar=20 μm; **b** bacteria in the intercellular space (*IS*), note the cell wall apposition (*arrow*), bar=0.5 μm; **c**, **d** bacteria in the intercellular space, note several bacterial morphotypes designed in **d** as *single* or *double arrows*, bar=2 and 0.5 μm in **c** and **d**, respectively. *CW* plant cell wall

that *Pba* could spread within tobacco plants by downward vascular translocation. This is consistent with our data which indicate that 1 day after inoculation of tobacco stems when symptoms of disease were barely evident even at the site of inoculation, *Pba* cells were already present in the roots of 50 % of the plants analysed (mean CFU value 7.4×10^2 CFU g^{-1}). On the second day after inoculation, when the symptoms were local and the macerated zone was 1–2 cm above the stem base, the root systems of all of the plants were colonised extensively, with a mean titre of 1.5×10^7 CFU g^{-1}.

Discussion

This report describes the life cycle of *Pba* within tobacco plants. Although potato is considered to be the exclusive host of *Pba*, we showed that this pathogen causes symptoms of typical tissue maceration in axenically grown tobacco. The symptoms of disease in the infected tobacco tissues were essentially distinct from the hypersensitive response (HR) because the affected area was not restricted to the inoculation zone. Instead, the necrosis spread both upward and downward from the site of inoculation, with the entire plant eventually becoming macerated (Fig. 1). Furthermore, the HR is known to restrict the propagation of bacteria within the plant, whereas the population of *Pba* inside tobacco plants increased considerably (up to four orders of magnitude compared with the cell quantity in the inoculum) during the course of disease development (Fig. 2).

Tobacco plants, but not potato plants (the normal host of *Pba* cells), were chosen to characterise the changes in microbial population during plant colonisation because our preliminary experiments indicated that the symptoms of tobacco plants that are infected with *Pba* vary considerably less than those that follow infection of potato with *Pba*. A similar variability in the symptoms of host plant symptoms in response to *Pba* was reported previously (Lapwood and Harris 1982; Adams and Lapwood 1983; Helias et al. 2000a; Helias et al. 2000b). The uniformity of disease development in tobacco makes this plant species relevant to elucidating the steps crucial to the interaction of *Pba* with plants.

Formation of VBN cells was detected in *Pba* populations after plant death. The VBN cells completely lost their colony-forming abilities, although they could be detected by real-time PCR (Fig. 2). Indisputable evidence of the viability of non-culturable *Pba* cells was their ability to be resuscitated. In order to restore the proliferative activity of living *Pba* cells (if any) from the plant remnants, we performed a number of procedures (see the "Material and methods" section), two of which were able to resuscitate *Pba* cells.

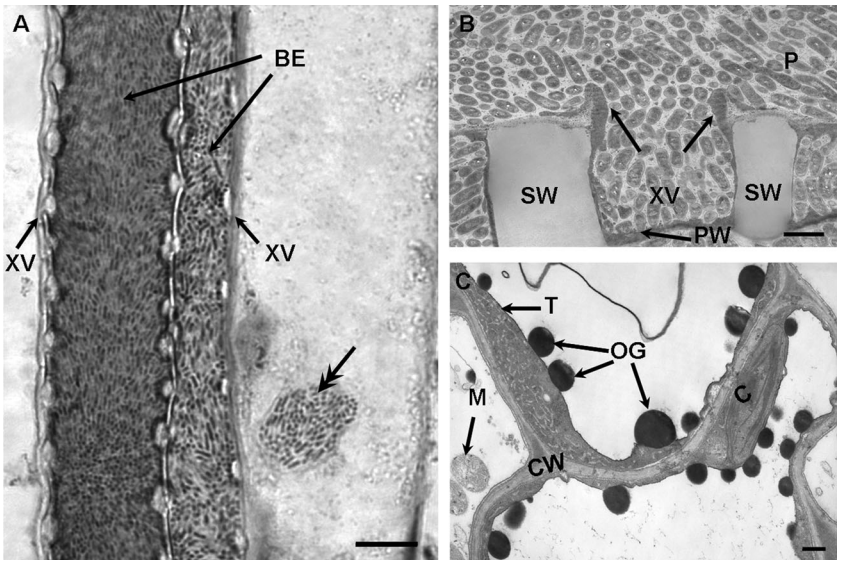

Fig. 7 Sections of tobacco stem 5–7 mm below the macerated zone, 2 dpi with *Pectobacterium atrosepticum* SCRI1043 (*Pba*). **a** Light microscopy, bacterial emboli (*BE*) in longitudinal section of xylem vessels (*XV*), note the release of bacterial mass to the adjacent parenchymatous cell (*double arrow*), bar=10 μm; **b** transmission electron microscopy, dissolution of primary cell wall (*arrows*) and bacterial transition from the xylem vessel to the adjacent parenchymatous cell, bar=2 μm; **c** transmission electron microscopy, osmiophilic globules (*OG*) in the vacuole of parenchymatous cells, bar=0.5 μm. *CW* cell wall, *PW* primary cell wall, *P* parenchymatous cell, *M* mitochondria, *C* chloroplast, *T* tonoplast, *SW* secondary cell wall of xylem vessel

Pba is common in moderate climates and can tolerate low temperatures at the end of the vegetative phase of the life cycle (Harris and Lapwood 1978; Perombelon and Kelman 1980; Lapwood and Harris 1982; Zimnoch-Guzowska et al. 1999). Accordingly, we attempted to imitate the natural environment by applying the freeze–thaw cycle to the remnants of infected plants, from which no CFUs were recovered before resuscitation. After freezing and thawing, the colony-forming capacities of 5 of the 30 samples analysed was restored immediately, with the colony-forming capacities of an additional 5 samples being restored 2 days later.

Three considerations suggest that the increase in the number of CFUs occurred as a result of the resuscitation of VBN cells, rather than regrowth of normal cells: (1) we used only plant residues for which no CFUs were detected before the resuscitation procedures; (2) for several samples, the increase of CFU titre that was observed immediately after the resuscitation procedures was too substantial and too rapid to be attributed to regrowth (from 0 to 5.3×10^3 to 1.7×10^6 CFU g^{-1} of plant debris within 2 h in some of the samples); (3) additional substrate was not added to support bacterial growth.

The transition into the VBN state is usually referred to as an adaptive programme, which enables bacteria to retain a reserve population under unfavourable conditions (Rahman et al. 1996; Day and Oliver 2004). Although VBN cells were reported for a variety of bacterial species, most of the investigations were carried out either in vitro or involved the use of animal model systems, and the occurrence of VBN cells of plant pathogenic bacteria *in planta* has only been described few times (Grey and Steck 2001; Ordax et al. 2009). Like *Ralstonia solonacearum* cells, *Pba* cells are transformed into a dormant state after death of the host plant. However, the colony-forming ability in *R. solonacearum* VBN cells could be restored by the addition of host-derived compounds, which have been suggested to provide a resuscitation signal (Grey and Steck 2001). In *Pba*, no resuscitation of VBN cells was observed after the addition of plant extract. Restoration of the colony-forming ability of *Pba* VBN cells was observed after either washing cells or subjecting them to a freeze–thaw cycle. The VBN state of *Pba* cells warrants further characterisation, given that it can promote the survival of soil bacteria at relatively low temperatures and thus ensure that plants can be infected during the subsequent vegetative season.

Ultrastructural alterations observed in parenchymatous cells in response to *Pba* infection included the formation of membrane structures that enveloped the bacterial cells (Fig. 3f), the formation of osmiophilic globules in the vacuoles (Figs. 3c and 7c) and the modification of organelles and cell compartments (Fig. 3e). Bacteria that cause soft rot are often regarded as intercellular pathogens that do not penetrate plant cells. However, in addition to being observed in the apoplast, *Pba* were observed inside parenchymatous cells of tobacco plants (Fig. 3c–f). Since the abovementioned ultrastructural modifications of parenchymatous cells (formation of osmiophilic globules and membrane structures) were pathogen-induced and were accompanied by a relatively low amount of *Pba* cells present within the parenchyma, we assumed that they might temporarily restrict bacterial propagation in the parenchyma, especially inside the cells. At the same time, granular substances originating from the vessel cell

walls (Fig. 4a, b) neither caused visible bacterial damage nor restricted their multiplication within the xylem vessels. Thus, different substances found in the infected plants (granular substances and osmiophilic globules) originating from different plant compartments (vessel cell walls and the vacuoles of parenchymatous cells, respectively) are likely to have a different impact on the *Pba* propagation.

During the acute stage of infection, *Pba* multiplication was more pronounced in the intercellular spaces than inside the cells. When tissue maceration was apparent, the parenchyma was colonised heavily by bacteria with a typical cellular ultrastructure; plant cells at this stage suffered significant damage.

After plant death, the parenchyma-localised *Pba* cells assumed a morphology different from that of *Pba* cells within living plant tissues. Some of the *Pba* cells resembled VBN cells (Fig. 6c, d), which were characterised in vitro in our previous work (Gorshkov et al. 2009). This is in agreement with the presented data obtained by plating experiments, real-time PCR (Fig. 2) and experiments to optimise resuscitation procedures, which demonstrated the transformation of *Pba* cells to the VBN state within the remnants of dead plants.

Colonisation of xylem vessels was coupled with the formation of complex structures, which we have named bacterial emboli. The term "emboli" refers to the extrinsic formations that occlude vessels and is frequently used to describe air bubbles that block the transport of either water or blood. Bacterial emboli block vessels by forming specialised and structured bacterial clumps. In contrast to biofilms, which usually have channels essential for liquid circulation, bacterial emboli did not have channels and were constructed as dense structures (Fig. 4g–i). Bacterial cells within the emboli were packed tightly and had a predominant orientation (along the long axis of the xylem vessel; Fig. 4d, h). There were also differences in the major steps involved in the formation of biofilms and bacterial emboli. Whereas bacterial attachment to a surface is crucial for the formation of biofilm (Purcell and Hopkins 1996; Danhorn and Fuqua 2007; Baccari and Lindow 2011), no attachment of bacterial cells to the vessel cell wall has been revealed during the assemblage of bacterial emboli (Fig. 4 a–c). This is consistent with the poor biofilm-forming capacity of *Pba*, which was reported recently (Perez-Mendoza et al. 2011). The formation of bacterial emboli was related to the release of substances from the vessel cell wall (Fig. 4a), which gave rise to a gel in which bacteria were trapped (Fig. 4b–d). Moreover, during the formation of emboli, bacteria were attached to each other through pilus-like structures (Fig. 4e), which together with the formation of gel resulted in the assembly of a bacterial embolus and complete occlusion of the vessel (Fig. 4h and 7a).

The formation of bacterial emboli in xylem vessels may affect water exchange in these vessels. This, in turn, may provide conditions that promote downward translocation of *Pba* through the xylem vessels. In our experiments, *Pba* cells after stem inoculation reached the roots relatively quickly (within 1–2 days after inoculation). At that time, parenchyma below the inoculation zone was not invaded by bacteria, whereas xylem vessels were colonised intensively. That indicates the downward movement of bacteria through the xylem vessels.

Translocation of bacteria internally through xylem vessels from aerial plant parts to underground plant parts has also been described for several bacterial species, including those that cause soft rot (Wallis et al. 1973; Boher et al. 1995; Czajkowski et al. 2010; Misas-Villamil et al. 2011). We propose that the formation of bacterial emboli stops the upward flow of water through xylem vessels and creates conditions that promote the downward translocation of microorganisms to enable them to colonise underground plant parts.

Conclusions

Our study shows that bacterial population within plants is not a set of similar microbial cells but should instead be regarded as a structured developing system. Bacteria interact with different plant tissues in different ways, resulting in the dissociation of microbial populations and the formation of various subpopulations, which are likely to be crucial for plant colonisation and passage through the bacterial population cycle. The bacterial emboli described here are an example of such a specialised subpopulation. These structured bacterial clumps are formed in the xylem vessels and lead to their occlusion. They are composed of tightly packed bacterial cells having a predominant spatial orientation and have a peculiar way of formation. After plant death, *Pba* cells persist in the VBN state, and their capacity to form colonies can be restored after resuscitation.

Acknowledgments This study was supported in part by the Russian Foundation for Basic Research, research project nos. 12-04-31059-MOL_A and 11-04-02097-a and by a grant from the programme Leading Scientific Schools no. NSH-825.2012.4 (Supervisor A.N. Grechkin) and grant no. 14.740.11.1190 from the Federal Target Programme.

Conflict of interest The authors declare that they have no conflict of interest.

References

Adams MJ, Lapwood DH (1983) The effect of *Erwinia carotovora* subsp. *atroseptica* (blackleg) on potato plants. II. Compensatory growth. Ann Appl Biol 103:79–85

Anetzberger C, Pirch T, Jung K (2009) Heterogeneity in quorum sensing-regulated bioluminescence of *Vibrio harveyi*. Mol Microbiol 73: 267–277

Baccari C, Lindow SE (2011) Assessment of the process of movement of *Xylella fastidiosa* within susceptible and resistant grape cultivars. Phytopathol 101:77–84

Barnard AML, Bowden SD, Burr T, Coulthurst SJ, Monson RE, Salmond GPC (2007) Quorum sensing, virulence and secondary metabolite

production in plant soft-rotting bacteria. Phil Trans R Soc B 362: 1165–1183

Bell KS, Sebaihia M, Pritchard L, Holden MTG, Hyman LJ, Holeva MC, Thomson NR, Bentley SD, Churcher LJC, Mungall K, Atkin R, Bason N, Brooks K, Chillingworth T, Clark K, Doggett J, Fraser A, Hance Z, Hauser H, Jagels K, Moule S, Norbertczak H, Ormond D, Price C, Quail MA, Sanders M, Walker D, Whitehead S, Salmond GPC, Birch PRJ, Parkhill J, Toth IK (2004) Genome sequence of the enterobacterial phytopathogen *Erwinia carotovora* subsp. *atroseptica* and characterization of virulence factors. Microbiology 101:11105–11110

Boher B, Kpemoua K, Nicole M, Luisetti J, Geiger JP (1995) Ultrastructure of interactions between *Cassava* and *Xanthomonas campestris* pv. *manihotis*: cytochemistry of cellulose and pectin degradation in a susceptible. Phytopathol 85:777–788

Christensen L, Moser C, Jensen P, Rasmussen T, Christophersen L, Kjelleberg S, Kumar N, Hoiby N, Givskov M, Bjarnsholt T (2007) Impact of *Pseudomonas aeruginosa* quorum sensing on biofilm persistence in an *in vivo* intraperitoneal foreign-body infection model. Microbiol 153:2312–2320

Collmer A, Keen NT (1986) The role of pectic enzymes in plant pathogenesis. Ann Rev Phytopathol 24:383–409

Cui Y, Madi L, Mukherjee A, Dumenyo CK, Chatterjee AK (1996) The RsmA$^-$ mutants of *Erwinia carotovora* subsp. *carotovora* strain Ecc71 overexpress $hrpN_{Ecc}$ and elicit a hypersensitive reaction-like response in tobacco leaves. MPMI 9:565–573

Czajkowski R, de Boer WJ, van Veen JA, van der Wolf JM (2010) Downward vascular translocation of a green fluorescent protein-tagged strain of *Dickeya* sp. (Biovar 3) from stem and leaf inoculation sites on potato. Phytopathol 100:1128–1137

Danhorn T, Fuqua C (2007) Biofilm formation by plant-associated bacteria. Annu Rev Microbiol 61:401–422

Day AP, Oliver O (2004) Changes in membrane fatty acid composition during entry of *Vibrio vulnificus* into the viable but nonculturable state. J Microbiol 42:69–73

Duda VI, Pronin SV, El'-Registan GI, Kaprel'iants AS, Mitiushina LL (1982) Formation of resting refractile cells in *Bacillus cereus* as affected by an autoregulatory factor. Mikrobiologiia 51:77–81

El'-Registan GI, Muliukin AL, Nikolaev IA, Suzina NE, Gal'chenko VF, Duda VI (2006) Adaptive functions of extracellular autoregulators of microorganisms. Mikrobiologiia 75:446–456

El'-Registan GI, Tsyshnatii GV, Duzha MV, Pronin SV, Mitiushina LL (1980) Regulation of growth and of *Pseudomonas carboxydoflava* by specific endogenous factors. Mikrobiologiia 49:561–565

Ger MJ, Chen CH, Hwang SY, Huang HE, Podile AR, Dayakar BV, Feng TY (2002) Constitutive expression of *hrap* gene in transgenic tobacco plant enhances resistance against virulent bacterial pathogens by induction of a hypersensitive response. MPMI 15:764–773

Gorshkov V, Petrova O, Gogoleva N, Gogolev Y (2010) Cell-to-cell communication in the populations of enterobacterium *Erwinia carotovora* ssp. *atroseptica* SCRI1043 during adaptation to stress conditions. FEMS Immunol Med Microbiol 59:378–385

Gorshkov VY, Petrova OE, Mukhametshina NE, Ageeva MV, Mulyukin AL, Gogolev YV (2009) Formation of "nonculturable" dormant forms of the phytopathogenic enterobacterium *Erwinia carotovora*. Mikrobiologiia 78:585–592

Grey B, Steck T (2001) The viable but nonculturable state of *Ralstonia solanacearum* may be involved in long-term survival and plant infection. Appl Environ Microbiol 7:3866–3872

Harris RI, Lapwood DH (1978) The spread of *Erwinia carotovora* var. *atroseptica* (blackleg) from degenerating seed to progeny tubers in soil. Potato Res 21:285–294

Helias V, Andrivon D, Jouan B (2000a) Development of symptoms caused by *Erwinia carotovora* ssp. *atroseptica* under field conditions and their effects on the yield of individual potato plants. Plant Pathol 49:23–32

Helias V, Andrivon D, Jouan B (2000b) Internal colonization pathways of potato plants by *Erwinia carotovora* ssp. *atroseptica*. Plant Pathol 49:33–42

Huang P-Y, Huang J-S, Goodman RN (1975) Resistance mechanisms of apple shoots to an avirulent strain of *Erwinia amylovora*. Physiol Plant Pathol 6:283–287

Kim H-S, Thammarat P, Lommel SA, Hogan CS, Charkowski AO (2011) *Pectobacterium carotovorum* elicits plant cell death with DspE/F but the *P. carotovorum* DspE does not suppress callose or induce expression of plant genes early in plant–microbe interactions. MPMI 24:773–786

Kussell E, Leibler S (2005) Phenotypic diversity, population growth, and information in fluctuating environments. Science 309:2075–2078

Lapwood DH, Harris RI (1982) The spread of *Erwinia carotovora* subsp. *atroseptica* and subsp. *carotovora* from stem lesions and degenerating seed tubers to progeny tubers in soil. Potato Res 25:41–50

Lidstrom M, Konopka M (2010) The role of physiological heterogeneity in microbial population behavior. Nature Chem Biol 6:705–712

Lin K, Husmeier D, Dondelinger F, Mayer CD, Liu H, Prichard L, Salmond GPC, Toth IK, Birch PRJ (2010) Reverse engineering gene regulatory networks related to quorum sensing in the plant pathogen *Pectobacterium atrosepticum*. Methods Mol Biol 673:253–81

Liu H, Coulthurst SJ, Pritchard L, Hedley PE, Ravensdale M, Humphris S, Burr T, Takle G, Brurberg M-B, Birch PRJ, Salmond GPC, Toth IK (2008) Quorum sensing coordinates brute force and stealth modes of infection in the plant pathogen *Pectobacterium atrosepticum*. PLoS Pathogens 4:1–11

Liu Y, Jiang G, Cui Y, Mukherjee A, Ma W, Chatterjee A (1999) kdgREcc negatively regulates genes for pectinases, cellulase, protease, harpinEcc, and a global RNA regulator in *Erwinia carotovora* subsp. *carotovora*. J Bacteriol 181:2411–2422

Mäe A, Montesano M, Koiv V, Palva ET (2001) Transgenic plants producing the bacterial pheromone *N*-Acyl-homoserine lactone exhibit enhanced resistance to the bacterial phytopathogen *Erwinia carotovora*. MPMI 14:1035–1042

Manos J, Arthur J, Rose B, Bell S, Tingpej P, Hu H, Webb J, Kjelleberg S, Gorrell M, Bye P, Harbour C (2009) Gene expression characteristics of a cystic fibrosis epidemic strain of *Pseudomonas aeruginosa* during biofilm and planktonic growth. FEMS Microbiol Lett 292:107–114

Mattinen L, Nissinen R, Riipi T, Kalkkinen N, Pirhonen M (2007) Host-extract induced changes in the secretome of the plant pathogenic bacterium *Pectobacterium atrosepticum*. Proteomics 7:3527–3537

Matz M, McDougald D, Moreno A, Yung P, Yildiz F, Kjelleberg S (2005) Biofilm formation and phenotypic variation enhance predation-driven persistence of *Vibrio cholerae*. PNAS 102:16819–16824

Misas-Villamil JC, Kolodziejek I, van der Hoorn RAL (2011) *Pseudomonas syringae* colonizes distant tissues in *Nicotiana benthamiana* through xylem vessels. Plant J 67:774–782

Muliukin AL, Lusta RF, Griaznova MN, Kozlova AN, Duda VI, El'-Registan GI (1996) Formation of a resting form of *Bacillus cereus* and *Micrococcus luteus*. Mikrobiologiia 65:782–789

Muliukin AL, Suzina NE, Duda VI, El'-Registan GI (2008) Structural and physiological diversity among cystlike resting cells of bacteria of the genus *Pseudomonas*. Mikrobiologiia 77:512–23

Murashige T, Skoog F (1962) A revised medium for rapid growth and bio assays with tobacco tissue cultures. Physiol Plant 15:473–497

Oliver J (1995) The viable but non-culturable state in the human pathogen *Vibrio vulnificus*. FEMS Microbiol Lett 133:203–208

Ordax M, Biosca EG, Wimalajeewa SC, López MM, Marco-Noales E (2009) Survival of *Erwinia amylovora* in mature apple fruit calyces through the viable but nonculturable (VBNC) state. J Appl Microbiol 107:106–116

Perez-Mendoza D, Coulthurst SJ, Sanjuan J, Salmond GPC (2011) *N*-Acetylglucosamine-dependent biofilm formation in *Pectobacterium atrosepticum* is cryptic and activated by elevated c-di-GMP levels. Microbiology 157:3340–3348

Perombelon MCM, Kelman A (1980) Ecology of the soft rot *Erwinias*. Annu Rev Phytopathol 18:361–387

Purcell AH, Hopkins DL (1996) Fastidious xylem-limited bacterial plant pathogens. Annu Rev Phytopathol 34:131–151

Rahman I, Shahamat M, Chowdhury M, Colwell R (1996) Potential virulence of viable but nonculturable *Shigella dysenteriae* type I. Appl Environ Microbiol 62:4621–4626

Ramey B, Koutsoudis M, von Bodman S, Fuqua C (2004) Biofilm formation in plant–microbe associations. Curr Opin Microbiol 7:602–609

Reynolds ES (1963) The use of lead citrate at high pH as an electron opaque stain in electron microscopy. J Cell Biol 17:208–212

Roszak D, Grimes D, Colwell R (1984) Viable but nonrecoverable stage of *Salmonella enteritidis* in aquatic systems. Can J Microbiol 30:334–338

Sambrook J, Fritsch EF, Maniatis T (1989) Molecular cloning: a Laboratory Manual, Second Edition. Cold Spring Harbor Press, Cold Spring Harbor, NY, p 1659

Stoodley L, Stoodley P (2009) Evolving concepts in biofilm infection. Cell Microbiol 11:1034–1043

Suzina NE, Muliukin AL, Kozlova AN, Shorokhova AP, Dmitriev VV, Barinova ES, Mokhova ON, El'-Registan GI, Duda VI (2004) Ultrastructure of resting cells of some non-spore-forming bacteria. Mikrobiologiia 73:516–529

Tang X, Hiao Y, Zhou JM (2006) Regulation of the type III secretion system in phytopathogenic bacteria. MPMI 19:1159–1166

Thiery JP (1967) Mise en evidence des polysaccharides sur coupes fines en microscopie electronique. J Microsc 6:987–1018

Wallis FM, Rijkenberg FHJ, Joubert JJ, Martin MM (1973) Ultrastructural histopathology of cabbage leaves infected with *Xanthomonas campestris*. Physiol Plant Pathol 3:371–378

Zimnoch-Guzowska E, Lebecka R, Pietrak J (1999) Soft rot and blackleg reactions in diploid potato hybrids inoculated with *Erwinia* spp. Amer J Potato Res 76:199–207